Silicon (2021) 13:2041–2052
https://doi.org/10.1007/s12633-020-00583-2

ORIGINAL PAPER

Gate All Around Junctionless Dielectric Modulated BioFET Based Hybrid Biosensor

Design, Simulation and Performance Investigation

Nawaz Shafi[1] · Jaydeep Singh Parmaar[1] · Ankita Porwal[1] · Aasif Mohammad Bhat[1] · Chitrakant Sahu[1] · C. Periasamy[1]

Received: 29 February 2020 / Accepted: 30 June 2020 / Published online: 18 July 2020

Abstract

Here in this work, we demonstrate the concept of hybrid biosensor based on embedded cavity gate all around (GAA) junctionless field effect transistors (JLT) capable of sensing, amplification and noise cancellation simultaneously for the first time. The disadvantages of low sensitivity and noise in classical concept of single device biosensor system are mitigated using a hybrid scheme, where sensing is performed by p-type and n-type FETs simultaneously. The proposed hybrid biosensor is designed by exploiting dielectric modulation property of embedded nanogap cavity biologically sensitive field effect transistors (DM-FETs). Lookup table (LUT) based Verilog-A models are developed for p and n type devices considering various types of biosamples in the embedded nanogap cavity. The developed Verilog-A models are imbibed into Cadence Virtuoso to perform the circuit simulations. The biomolecules are simulated as dielectric materials with different permitivities in the embedded nanogap cavity. The proposed hybrid biosensor has been analyzed for different topologies and performance comparisons have been carried out between junctionless based DM-FET and inversion mode DM-FET based biosensors. The performance of proposed DM-FET based hybrid biosensor has been evaluated through voltage transfer characteristics (VTCs) in terms of logic threshold voltage shift ($\triangle V_{Lt}$) and gain (A_V). Performance comparisons for different topologies including resistive load, single stage and cascaded two stage hybrid biosensors have also been analyzed. Cascaded GAA JLT configured biosensors yields the highest $\triangle V_{Lt}$ sensitivity of 61.14%. However the results emphasize the superior all-round performance of cascaded CMOS configuration with $\triangle V_{Lt} \simeq 30\%$ and gain $A_V = 55$.

Keywords BioFET · Dielectric modulation · Embedded cavity · Gate all around (GAA) · Junctionless transistor (JLT) · Logic threshold voltage · Sensitivity · Voltage transfer characteristic (VTC).

1 Introduction

The utilization of novel semiconductor technologies for development of biosensors have created a positive impact in healthcare, clinical screening and medical diagnosis [1]. The classical methods for biosensing have catered the demands with varied success rate where the failures in general are owed to indirect sensing mechanism. One of the prominent features of nanotechnology is unmediated label free detection of biomolecules intended for super-sensitive, reliable, and low power consuming biomolecule detection devices. The variation in concentration of biomolecules such as proteins, lipids, nucleic acids etc in human body is related to presence or development of a disease. Detection of such biomolecules gives doctors a quantitative basis for clinical treatment approach [2]. Numerous biosensing devices based on different techniques have been proposed including optoelectronic based, piezoelectricity based, MEMS based, potentiometric based, FET based [3]. In the midst of listed sensing technologies, semiconductor biosensors including nanowires and BioFETs have proven to be efficient candidates for point of care (POC) testing and diagnosing systems. BioFETs outclass other sensing techniques due to advantages which include direct transduction of chemical quantity to equivalent electrical

✉ Nawaz Shafi
2017rec9021@mnit.ac.in

[1] Department of Electronics and Communucation Engineering, Malaviya National Institute of Technology Jaipur, Rajasthan, 302017, India

quantity for read-out and processing, cost effective due to mass production and high integration density, and label free detection [4]. Most of FET based biosensors require tedious surface functionalization steps for detection leading to increase in cost, complexity and necessity of skilled operators [5].

Ion-sensitive field effect transistor (ISFET) is first of the kind FET biosensors earlier proposed for pH sensing [6]. The solid-state gate electrode structure was modified into liquid gate where measurements were carried using reference electrode. ISFETs was latter modified for applications in diverse areas outlined by Schoning and Poghossian [7]. The process of biomolecule immobilization is accomplished by complete immersion of ISFETs in electrolyte leading to indeterministic statistical fluctuations in measurements. ISFETs inherently show unpredictable operational etiquette which include drift [8], hysteresis [9]. Drift is induced by unstable reference electrode potential which fluctuates with operational leakage currents and surrounding temperature fluctuations [10].

Choi et. al. in 2007 modified the conventional silicon on insulator (SOI) MOSFET structure forming nanogap cavities by etching part of sacrificial gate metal for lodging biomolecules. The nanogaps can also be formed by etching a sufficiently thick ($>$ 5 nm) gate oxide [11]. The formation of nanogaps elevates the threshold voltage (V_T), and on subsequent occupation by biomolecules, V_T is lowered according to dielectric constant of biomolecules. Dielectric modulated FETs have potential advantages of detecting weakly charged and neutral over ISFETs with comparable sensitivity, selectivity and linearity [12, 13]. Despite of being advantageous, DMFET suffers from physical vulnerability due to partial suspended gate structure. The other limitations of DMFETs include alignment mismatch. The dielectric modulated FETs detect biomolecules that are feebly charged or neutral, hence the sensitivity is low. The biomolecules when lodged in the nanogap after functionalization alter the effective gate capacitance, causing threshold voltage (V_T) of the device to shift. The classical equation ($V_T = V_{FB} + 2\Phi + \frac{Q_{dep}}{C_{ox}}$) holds true for homogeneous gate oxide device. On cavity formation, $C_{eff,g}$ under the cavity changes causing V_T of entire device to shift as a function of permitivity of biomolecules in the cavity. The modulation in effective gate capacitance by dielectric permitivity of biomolecules affects the VT. This controls the transfer characteristics hence the current of the device [13].

Dielectric modulated BioFETs have a potential of being used as label-free sensors for rapid detection of bacteria, protein with sufficiently high sensitivity and small limit of lower detection . A considerable number of dielectric modulated BioFETs have been fabricated by different research groups in recent past and employed for detection of biomolecules such as biotin-streptavidin [14] , protein molecules [11], avian influenza [15], DNA charge [16], peptide nucleic acid (PNA) [17]. As reported in [18], such BioFETs shows high sensitivity and selectivity as compared to other BioFET architectures and also has ability to detect weakly charged molecules which is a limitation of ISFET. DM-BioFETs can be fabricated by fabrication scheme aligned to generic CMOS process.

During recent years, various structural modifications were reported for DMFET based biosensors for enhancing the sensing action of discrete transducer components [17, 19]. The strategic structural improvisation of device using novel junctionless doping profile mechanism throughout source-channel-drain of the transistor leading to minimization of short channel effects has already been reported [20]. Uniform doping throughout source channel and drain regions improves subthreshold slope and threshold voltage roll off. Conventional MOS devices for biosensors are not giving much promising results at lower technology node (below 180nm) due to incessant scaling effects. At lower technology nodes, MOS devices suffer from complexity in fabrication process and small geometry effects in general [21]. At device level from technology perspective, junctionless (JL) devices favor simpler fabrication process when correlated to conventional inversion mode devices due to deprivation of abrupt doping profiles [22]. In comparison to conventional inversion mode (IM) devices, a disparate conduction mechanism is perceived in JL devices as the current for gate voltage less than the threshold voltage (V_T) flows through the central axis of the majorly depleted body while for a gate voltage higher than flatband voltage (V_{FB}) creates an accumulated channel available for conduction [23]. This as a whole upsets the DC performance characteristics os the device particularly threshold voltage (V_T) and mobility (μ) [24]. Besides better gate control on channel which almost ceases the flow of Off current (I_{Off}), gate all around junctionless transistors show immunity to low frequency noise (1/f) noise which is a major reliability concern in FET biosensors [25]. There are two kinds of noise sources in junctionless devices: one is due to channel thickness fluctuations in the depletion region and the other is due to carrier concentration fluctuation at the oxide semiconductor interface in the accumulation region. Due to a symmetrical structure with gate wrapped all around junctionless architecture, additional trap and release of charge carriers will take place with formation of accumulation region in channel at higher gate bias providing high noise immunity in the proposed device [26]. The junctionless transistors have matured for analog/RF applications [27], superior subthreshold logic devices and memory [28], and biosensing applications [12]. During last decade a variety of FET biosensors have been fabricated and characterized but due to poor sensitivity or complex process flow, the feasibility is quiet low.

On-chip integration and convenient read out circuit for BioFETs in general is of much importance for real time sensing and signal processing. However only few articles are available that have focused on simplifying the detection circuitry. In this context, very few complex readout circuit strategies have been proposed for FET based pH and ion sensing applications making the system bulkier [16, 29]. Thus, such design strategies restrict the ensemble performances of sensing units and also lead to escalated complexity in integration with digital micro-fluidic based lab-on-chip systems, which drives the need for CMOS compatible simple detection/readout circuitry for pH and ion sensing applications.

The functionality of embedded cavity DM-FET based biosensors depends on intonation of threshold voltage and drain current through the device instigated by the effect on gate oxide capacitance by biomolecules in the embedded cavity [11, 15]. This threshold voltage and current change is incited by the variability in density of states, activation of surface sites, buffer ionic strength and ionic composition of biomolecules [30]. In present scenario, such biosensing device strategies suffer from low yield that may be revamped by amplification of current change para mounting the enhancement in figure of merits of biosensor like limit of lower detection (LOLD), sensitivity, and linearity [31, 32]. Conventional IM FET biosensors are limited by poor SNR due to intrinsic fluctuations and uncontrollability of parameters affiliated to detection [33]. Buitrago et al, have implemented a SOI based junctionless device of 500nm channel length for ion detection in the subthreshold region of operation. However to detect lower concentration of biosamples, device dimensions need to be scaled down where optimal signal to noise ratio is achieved [22]. The dielectric modulation effect on drain current is more dominant over charge modulation property in the linear mode of operation [18].

1.1 Major Contributions of this work

Herein we propose the scheme for hybrid biosensor based on dielectric modulation property of embedded cavity BioFETs. The BioFETs were designed using junctionless FETs and inversion mode FETs for gate all around architecture. The major contributions of this work include:

1. The proposed hybrid biosensor is simulated considering different biomolecules in the nanogap cavity pertaining different permitivities. Look-up tables (LUTs) are formed for varied permitivities and the circuit level analysis are carried out using Verilog-A models formed using LUTs.
2. The performance evaluation of proposed biosensor is evaluated in-terms of logic threshold voltage shift ($\triangle V_{Lt}$) and gain (A_V). Linearity an important figure merit is investigated and slope, error of straight line fit is computed for proposed and counterpart hybrid biosensors.
3. This work also carries out the performance analysis of proposed hybrid biosensor based on junctionless DM-FETS and conventional inversion mode FETs.

This paper is organized as follows. Section 2 discusses the design considerations and simulation and modeling framework for the proposed work. The subsequent sub-sections elaborate the concept and implementation. In Section 3 discusses the implementation and comparative study of different topologies for proposed concept. The conclusions from this work are presented in Section 4.

2 Concept, Design and Execution Methodology

2.1 Proposed Device Architecture and Design Constraints

Classical ion sensitive BioFETs are based on charge interaction at sensing membrane therefore are incapable for detection of weakly charged or neutral biomolecules [34]. Herein we present a improved architecture of a BioFET where weakly charged or neutral biospecies can be detected using embedded cavity based BioFET (DMFET). The gate all around (GAA) structure provides dual functionality including superior gate control on the channel and more cavity volume for lodging of biosample [35]. The cavity is realized by coercing a part of gate oxide or sacrificial gate metal through the process of etching. However classical embedded BioFET design suffer from limitations such as threshold voltage fluctuations, mechanical instability and thermal budget of doping process [17]. Abrupt junctions particularly at lower technology nodes are difficult to fabricate, and lead to significant leakage current accompanied by drain induced barrier lowering (DIBL). A junctionless (JL) high doping profile throughout the source-channel-drain regions yields significant improvements in subthreshold swing when proper gate material is used with enhanced drain current [12]. The 3D birds eye view of proposed device (gate all around embedded cavity dielectric modulated junctionless BioFET referred as GAA JLT) along with its cross sectional view is shown in Fig. 1. The performance of proposed device is compared to a similar classical doping profile structure (referred as GAA FET) at same technology node. The physical parameters for GAA JLT and GAA FET based BioFETs are listed in Table 1. An abrupt doping profile as a design consideration is used for conventional GAA FET based BioFET across

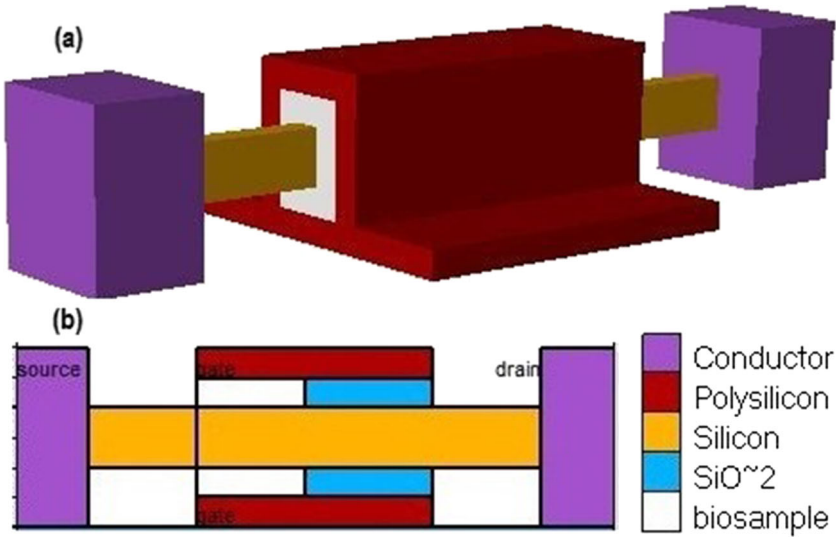

Fig. 1 **a** Three dimensional architecture schematic view of proposed dielectric modulated BioFET. **b** Corresponding cross-sectional view

source-channel and drain-channel junctions to account for worst case scenario of doping causing band to band tunneling leading to uncompromisable leakage current which is even worse for lower technology nodes.

The dimensions of cavity considered has been considered from fabrication perspective. BioFETs with cavity dimensions of as low as 15 nm × 200 nm [15] for avian influenza, 20nm × 2μ m [11] for DNA, 50 nm × 50 nm [17] for biotin, have been fabricated in recent past. The process for cavity formation falls in wet etch category of generic CMOS process using buffered oxide etch (BOE; HF:H2O = 1:6) or chromium etchant solution or selective vertical etch etc. [14, 15, 17]. Silicon is hydrophobic in nature but when silicon is exposed to air, a native oxide (SiO_2) layer is accumulated on the surface which is hydrophilic and has a tendency to attract aqueous solutions.

Table 1 Physical parameter specifications of proposed GAA JLT and GAA FET based DM-BioFETs

Parameter (Symbol)	Value
Gate length(L_g)	65 nm
Gate oxide thickness(T_{ox})	5 nm
Silicon thickness(T_{si})	10 nm
Silicon width(T_{si})	10 nm
Cavity length(L_{cavity})	30 nm
Cavity height(T_{cavity})	5 nm
Source spacer($L_{spac,S}$)	5 nm
Drain spacer($L_{spac,S}$)	5 nm
S/D length(L_s/L_d)	50 nm
Gate workfunction(ϕ_G (N/P))	4.1/5.25eV
Channel doping(N_{ch})	6×10^{15} cm^{-3}
Si Doping (P/N) (JL)(N_A/N_D)	1×10^{19} cm^{-3}
S/D Doping (P/N)(N_A/N_D)	$5 \times 10^{18}/5 \times 10^{19}$ cm^{-3}

This oxide layer acts as hydrophilic layer where functionalization takes place.Neutral biomolecules are non-reactive to dangling OH bonds of SiO_2 and effect the gate oxide capacitance by dielectric modulation property. The structure is analogous to stacked gate. To ensure that the current flowing in n type and p type device is equal, two p type devices were placed in parallel to account for W/L ratios. The cavity formed by etching is functionalized with specific biomolecule receptor agent which binds analyte in introduced sample. The interaction of receptor and target biomolecule alters the net dielectric constant of the nanogap [11, 15] . The biospecies lodged in the cavity after functionalization alter the effective gate capacitance (C_{Eff}), causing threshold voltage (V_T) of the device to shift. The classical equation ($V_T = V_{FB} + 2\Phi + \frac{Q_{dep}}{C_{ox}}$) holds true for homogeneous gate oxide device. On cavity formation, $C_{eff,g}$ under the cavity changes causing V_T of entire device to shift as a function of permitivity of biomolecules in the cavity [34].

The receptor-target binding in the cavity introduces a net polarization charge density hence the polarization field in the cavity in presence of the applied gate voltage. The electric field induced polarization field is different for neutral and charged biomolecules, but overall modifies the effective gate electric field and the charge carrier injection component in the channel. In conventional MOSFET based BioFET, at higher gate electric field the inversion charges in channel screen the electrostatic modulation of cavity due to polarization field from the channel. The maximum change in the drain current is observed in subthreshold mode of operation where the screening is much smaller comparatively. This follows that the desirable design consideration for BioFET includes less screening polarization field by the inversion charge density of channel at relatively higher gate bias [13].

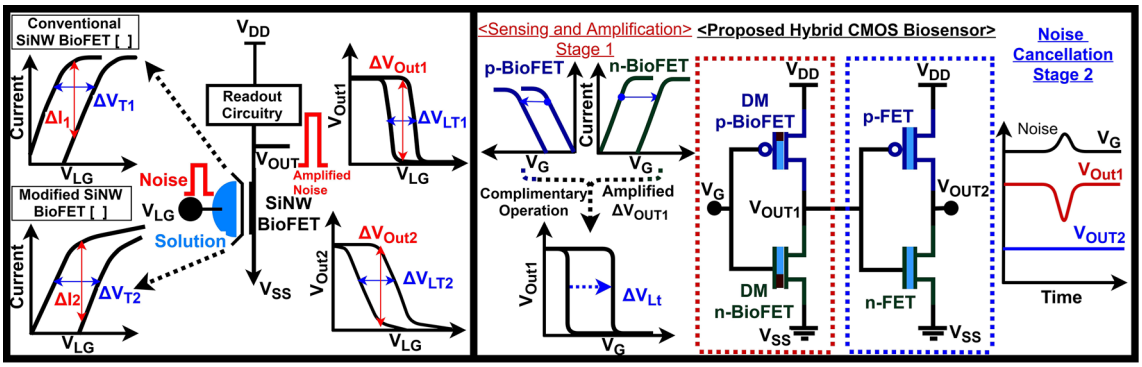

Fig. 2 **a** A single FET hybrid sensor where the current sensitivity can be improved by modifying the device architecture [36, 37], Although the current sensitivity increases yet such design are liable to noise amplification **b** Schematic of proposed concept and working of two stage hybrid biosensor involving bioresponse amplification and noise cancellation

2.2 Hybrid Biosensor: Design and Working

Classical biosensing strategy which involves a single detection BioFET has limited V_T shift as shown in Fig. 2a. Although, the V_T sensitivity can be improved by modifying the BioFET design (multi-gate architecture) but the current sensitivity is still a bottleneck, which limits the output voltage sensing margin. Figure 2a shows $\triangle V_{Out1} = \triangle V_{Out2}$ even if $\triangle V_{Lt2} > \triangle V_{Lt1}$. The increase in threshold voltage shift while maintaining output voltage same amplifies noise at the output. We propose a cascaded two stage biosensor design where sensing is accomplished by a pair of complimentary p-DMFET and N-DMFET simultaneously. This stage accomplishes sensing as well as amplification of the bioresponse (V_{OUT1}). The bioresponse from stage-1 (V_{OUT1}) is fed to series connected another complimentary pair which further amplifies the bioresponse and suppresses noise without mitigating sensitivity of the biosensor. The complete working diagram of proposed hybrid biosensor is shown in Fig.2b. The proposed hybrid biosensor system which comprises of two stages. First stage accomplishes sensing. The bio-response from first stage can be amplified using a p-FET loaded n-MOSFET amplifier on the same chip. This concept has been experimentally demonstrate and fabricated by generic CMOS aligned process by number of researchers in recent past for detection of pH, DNA, and protein [11, 14, 16]. Such hybrid devices are very much practical and feasible. The primary advantages include that an amplified bio-response is obtained in the electrical form from the sensing device itself making the processing very feasible.

The hybrid biosensor is implemented using proposed GAA JL-DMFET and performance has been compared to analogous GAA conventional DMFET. Different bio-molecules lodged in the functionalized in the nanogap cavity yield in shifted voltage transfer characteristics (different $\triangle V_{Lt}$) and gain. The shift in VTC and $\triangle V_{Lt}$ is quantified in the form of $\frac{\triangle V_{OUT1}}{\triangle K}$ a sensing metric for proposed biosensor. The change in logic threshold voltage with respect to change in permitivity of biomolecules ($\frac{\triangle V_{OUT1}}{\triangle K}$) is amplified by stage-2. The stage-wise change in gain is given in Table 2. Noise instigates a specific degree of uncertainty in detected signals. The indeterministic fluctuations in output bio-response can be falsely attributed to sensitivity, especially in cases where biosignal variation level is compared to level of fluctuations. The dominant sources of noise in nanodevice biosensors include thermally generated noise due motion of charge carriers in the channel, low frequency flicker (1/f) noise [26]. Previous studies in junctionless transistors especially with gate all around (GAA) structure show potential for extreme low noise level due to different charge carrier transport mechanism of bulk conduction than surface conduction in inversion mode devices. In junctionless nanowire transistor, $1/f$ noise is expected to originate due to bulk conduction fluctuations (Hooge mobility fluctuations) caused due to carrier scattering in the channel [35]. Due to a symmetrical structure with gate wrapped all around, additional trap and release of charge carriers will take place with formation of accumulation region in channel at higher gate bias [25].

2.3 Simulation Methodology and Framework

The simulation methodology consists of device simulations carrier out in Atlas device simulator. Quantum transport

Table 2 Output voltage sensitivity of stage-1 and stage-2 for CMOS hybrid biosensor

First stage

$$\frac{\triangle V_{out1}}{\triangle K} = \frac{\triangle V_{out1}}{\triangle V_G} \cdot \frac{\triangle V_G}{\triangle V_{Lt}} \cdot \frac{\triangle V_{Lt}}{\triangle K} \quad (1)$$

$$\frac{\triangle V_{out1}}{\triangle K} = A_{V1} \cdot 1 \cdot \frac{\triangle V_{Lt}}{\triangle K} \quad (2)$$

Second Stage

$$\frac{\triangle V_{out2}}{\triangle K} = \frac{\triangle V_{out2}}{\triangle V_{out1}} \cdot \frac{\triangle V_{out1}}{\triangle K} \quad (3)$$

$$\frac{\triangle V_{out2}}{\triangle K} = A_{V2} \cdot A_{V1} \cdot \frac{\triangle V_{Lt}}{\triangle K} \quad (4)$$

$$\frac{\triangle V_{out2}}{\triangle K} = A_{V2} \cdot A_{V1} \cdot \frac{\triangle V_{Lt}}{\triangle K} \quad (5)$$

device simulation have been carried out where Different models have been incorporated in Atlas device simulator that account for different phenomena taking place in the device. Field and concentration dependent mobility models along with Fermi-Dirac statistics have been used. The band gap narrowing model (BGN) have been invoked due to presence of highly doped silicon film. The device and circuit simulation methodology is shown in Fig. 3. As no standard SPICE models are available for junctionless devices at this technology node (65nm), look up table (LUT) based Verilog-A models have been developed which are latter employed for circuit simulations. The behavioral Verilog-A code interpolates the data of specific device for particular biomolecules from LUT for accurate value of current of corresponding applied biases.

The dimensions of the proposed DM-BioFET has been chosen carefully such that the biomolecules considered can fit in the cavity. The biomolecules considered are less than 1nm in size with APTES (with K=2.63) and Biotin (with K=3.57) of size 0.9nm and 0.56nm respectively [28]. The experimental research shows that these biomolecules are feebly charged or neutral hence can be detected using their dielectric permitivity through dielectric modulation technique [24].

The current conduction in surrounding gate nanowire junctionless transistors takes place through the volume rather than surface conduction mechanism. The electron concentration in the silicon channel for N-type GAA JL-DMFET in depleted and enhanced modes is shown through contour plots in Fig. 4a and b. The junctionless based DMFET provides a more desirable I_{On}/I_{Off} ratio of 10^7 against 4×10^5 of inversion mode device leading to higher transconductance (g_m) in JL based DM-BioFETs as shown in Fig. 5. The flow of drain current is in direct correlation with surface potential of silicon channel which is modulated by effective gate capacitance ($C_{eff,g}$) where $C_{eff,g}$ is function of biomolecule permitivity)K) lodged in the cavity [11].

3 Result and Discussion

In sensing and amplifying stage of proposed biosensor, when voltage at input (V_G) is less than the logic threshold voltage (V_{Lt}) of hybrid DM-FET based hybrid biosensor, the voltage at output node (V_{OUT}) is at higher potential. For some V_G, the conductivity of N-type device increases rapidly causing V_{OUT} to decrease. Due to dielectric modulation property of DM-BioFETs, V_{Lt} is largely dependent on the permitivity (K) of the biomolecules in the cavity. The complementary pair of BioFETs for sensing simultaneously provide amplification. For the proposed hybrid biosensor, the sensitivity analysis is done for different types of biomolecules simulated by different dielectric materials for sweeping V_G. At low V_G (i.e. n-DM-BioFET is in OFF state), there will be a minimum discharge of current to the ground. The discharge of current will be higher in conventional inversion mode device based biosensor due to higher magnitude order of Off current

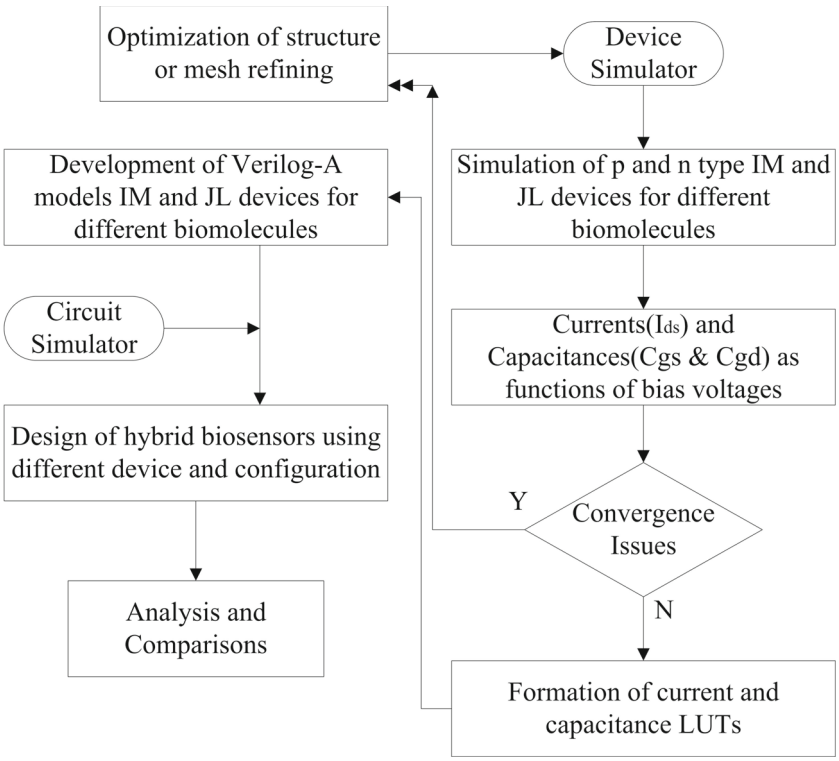

Fig. 3 Simulation and modeling methodology of proposed biosensor

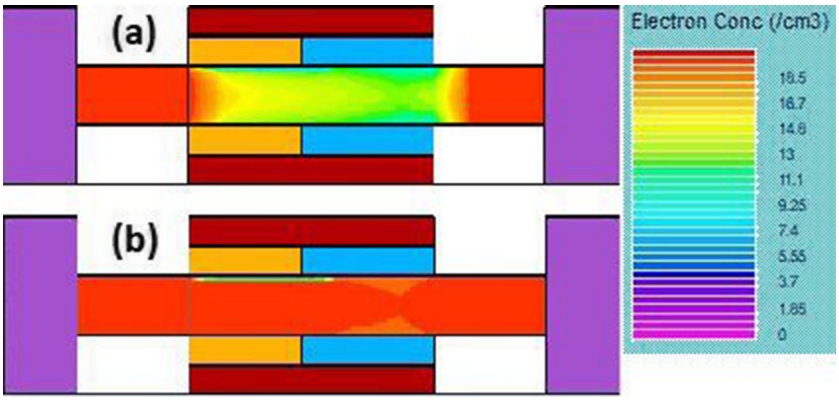

Fig. 4 Contour plots for electron concentration in silicon for (a). Off condition ($V_{GS} = 0V$), (b). On condition ($V_{GS} = 1.2V$) with $K = 3.57$ (APTES) in cavity for GAA JL-DMFET, at $V_{DS} = 1.2V$

(I_{OFF}) than junctionless DM-BioFETs. The potential at output node of stage-1 (V_{OUT1}) is a function of current flowing through the devices from V_{DD} to ground. Higher transconductance in junctionless dm-BioFET imply larger I_{ON}/I_{OFF} than conventional inversion mode dm-BioFET as shown in Fig. 5.

The performance proposed hybrid CMOS biosensor is characterized by voltage transfer characteristics. We have compared the performance of proposed junctionless GAA DM-BioFET based hybrid biosensor to following analogous configurations:

1. Single stage resistive load.
2. Single stage CMOS configured.
3. Two stage resistive load.
4. Two stage CMOS configured.

A comparative sensitivity analysis for junctionless based FETs and conventional inversion mode FETs has been carried out for above configurations. Biomolecules in the cavity with higher dielectric constants have their VTC's shift to the left on voltage scale. A unique shift in V_{Lt} ($V_{Lt} = V_{gate}@V_{out} = \frac{V_{DD}}{2}$) is observed for different biomolecules such as biotin, streptavidin, APTES.

A single stage resistive load hybrid biosensor is designed using junctionless DM-FET and inversion DM-FET. The voltage transfer characteristics and gain curves are shown in Fig. 6(a-d). The use of a resistive load in single stage hybrid biosensor where single n-type DM-FET is used as sensor device shows low noise margins providing lesser gain at output. The comparative analysis shows improved noise margins in VTC's when junctionless DM-FET is used as sensor device.

A similar single stage biosensor is designed where the resistive load is replaced with a P-type DM-FET sensor device. In this configuration a complimentary approach is used, where sensing is simultaneously accomplished by p and n type devices. The VTC and gain curves for such configuration is shown in Fig. 7. The use of junctionless devices improves gain remarkably. A significant shift in V_{Lt} in case of CMOS configured using junctionless devices for different biomolecules making it highly sensitive than its counterpart inversion mode DM-FET based biosensor.

The characteristics for two stage resistive load hybrid biosensors is shown in Fig. 8, where comparison in performance has been carried out for junctionless and inversion mode devices. The noise margin is enhanced in second stage VTC than the first stage, however the noise margins are high in hybrid biosensor designed using junctionless DM-FETs. The reason of better noise margins shown of junctionless device based configurations is due to higher gain. Due to high I_{On}/I_{Off} ratio of GAA JL DM-FETs, a considerable improvement in gain at V_{OUT2}

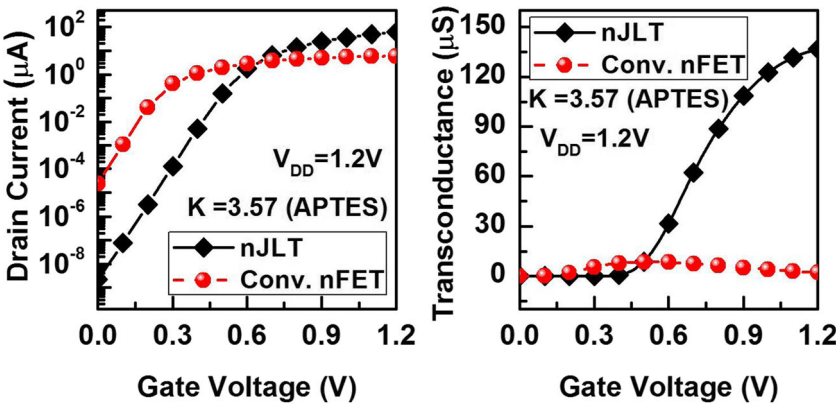

Fig. 5 a. I_{DS} vs V_{GS} characteristics for n-type junctionless and IM DM-BioFETs b. Transconductance (g_m) vs V_{GS} of n-type junctionless and IM DM-BioFETs for APTES (K = 3.57) in the embedded nanogap cavity. $V_{DD} = 1.2V$

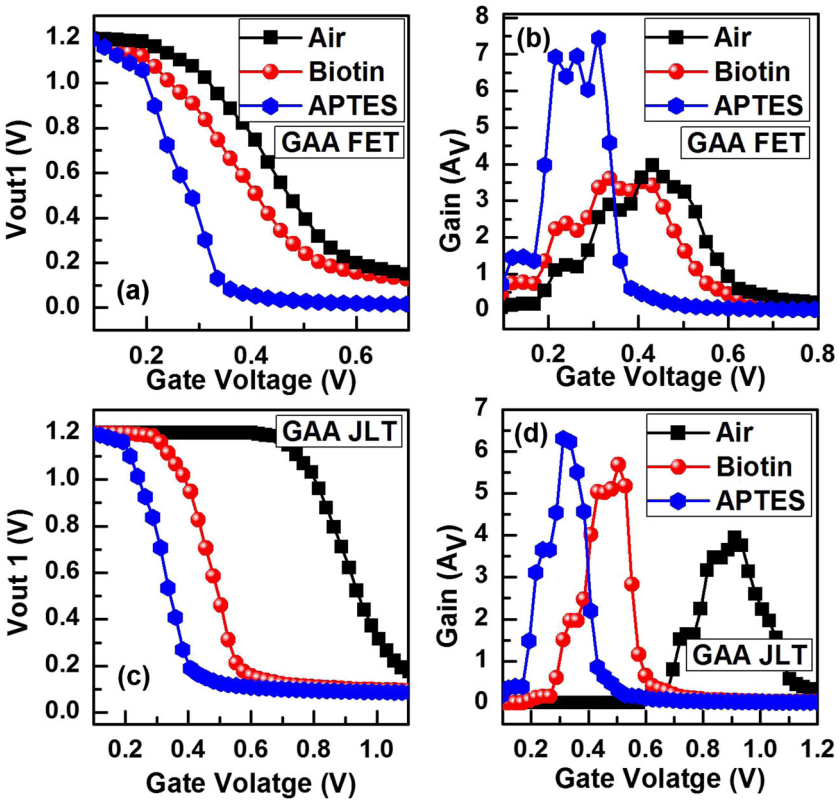

Fig. 6 (a-b). VTC and gain for GAA-IM DM-FET based single stage resistive load hybrid biosensor (c-d). Gain for GAA-JL DM-FET based single stage resistive load hybrid biosensor, $V_{DD} = 1.2V$

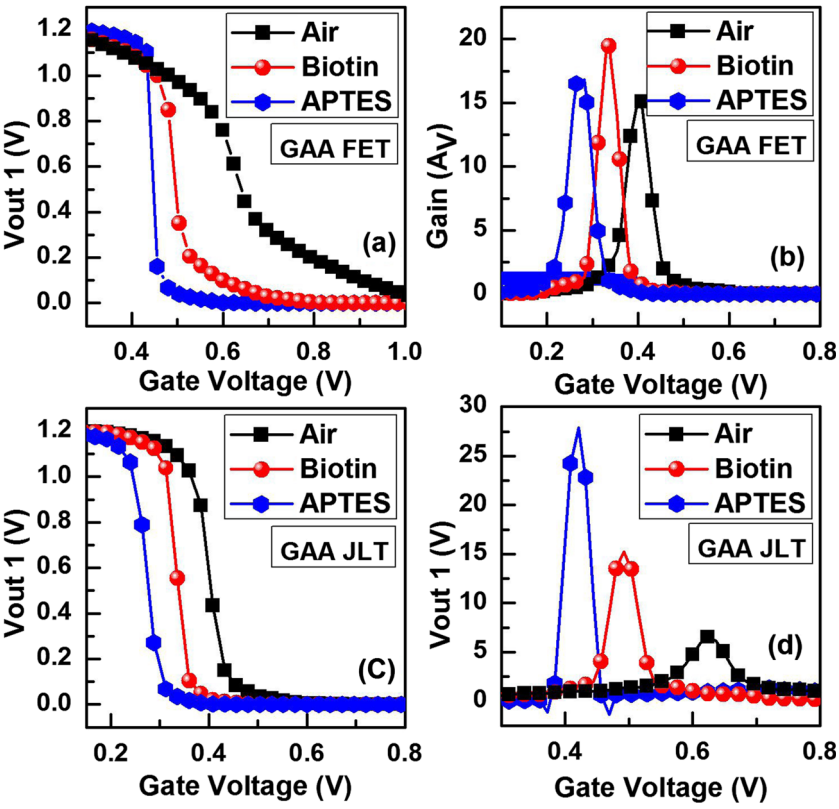

Fig. 7 (**a**-**b**). VTC and gain for GAA-IM DM-FET based single stage CMOS configured hybrid biosensor (**c**-**d**). Gain for GAA-JL DM-FET based single stage CMOS configured hybrid biosensor, $V_{DD} = 1.2V$

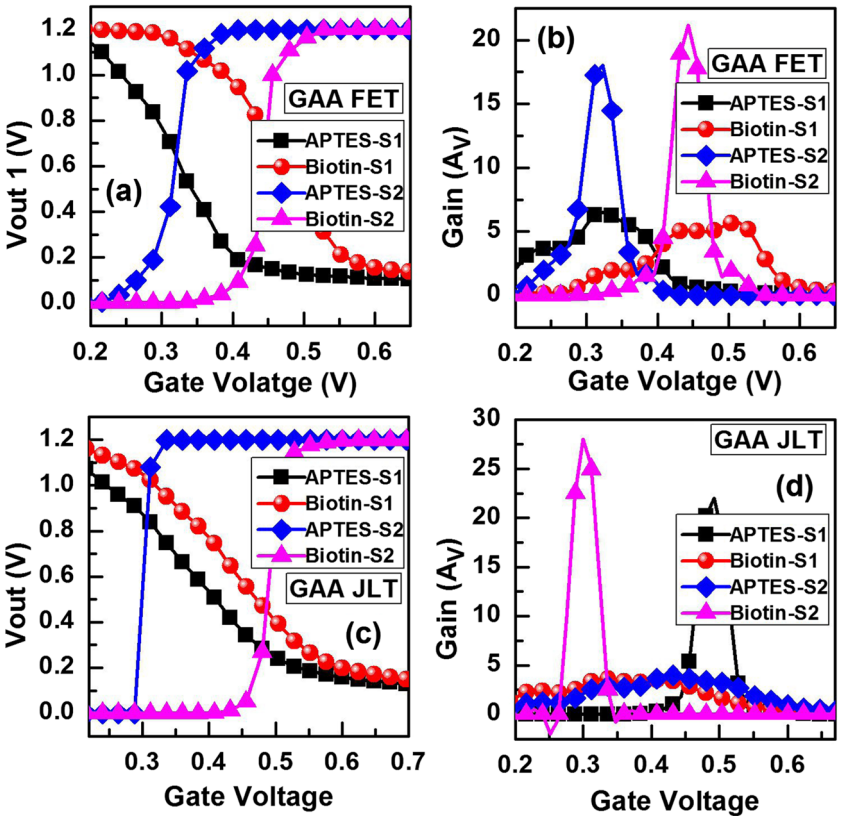

Fig. 8 (**a**-**b**). VTC and gain for GAA-IM DM-FET based two stage resistive load configured hybrid biosensor (**c**-**d**). Gain for GAA-JL DM-FET based two stage resistive load configured hybrid biosensor, $V_{DD} = 1.2V$. S1 and S2 represent stage-1 and stage-2 respectively

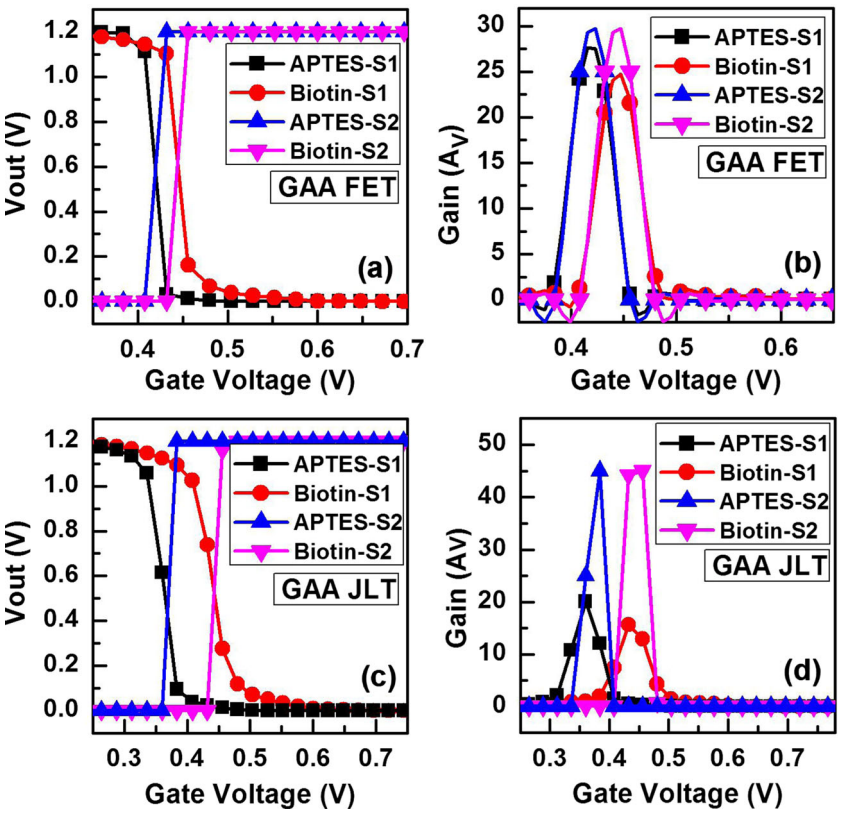

Fig. 9 (**a**-**b**). VTC and gain for GAA-IM DM-FET based two stage CMOS configured hybrid biosensor (**c**-**d**). VTC and Gain for GAAJL DM-FET based two stage CMOS configured hybrid biosensor, $V_{DD} = 1.2V$. S1 and S2 represent stage-1 and stage-2 respectively

Table 3 Tabular form of variations in gain (A_V) and logic threshold voltage (V_{Lt}) for different topologies of hybrid biosensor considering various biomolecules in the nanogap cavity assuming cavity to be fully occupied. The bottom 4 rows show performance metrics for cascaded two stage hybrid biosensors

Device	GAA IM DM-FET						GAA JL DM-FET					
Configuration	Resistive load			PFET load			Resistive load			PJLT load		
Driver	NFET			NFET			NJLT			NJLT		
Biomolecule	Empty	Biotin	APTES	Empty	Biotin	APTES	Empty	Biotin	APTES	Empty	Biotin	APTES
K	1	2.1	3.57	1	2.1	3.57	1	2.1	3.57	1	2.1	3.57
Logic $V_{Lt}(mV)$	420	370	260	650	500	420	900	510	320	430	320	270
Gain A_{V1}	4	3.7	7.5	15	19.5	17	4	5.8	6.5	7	15	27.5
$\triangle V_{Lt}(mV)$	–	50	160	–	150	230	–	390	580	–	110	160
% Sensitivity	–	11.8	39	–	25	37.4	–	45.4	65.4	–	24.45	35.65
Logic V_{Lt}(mV)	560	450	320	500	440	410	700	500	300	450	365	300
Gain A_{V2}	15	18	22	29	29	31	19	27	21	54	57	55
$\triangle V_{Lt}$(mV)	–	110	240	–	60	90	–	200	400	–	85	150
% Sensitivity	–	21.64	44.85	–	13.5	19.7	–	29.5	61.14	–	21.87	32

is achieved. Apart from such advantages, junctionless FETs are process voltage temperature(PVT) variation aware devices that make them immune to short channel effects effects making them robust for biosensing applications. The trend of relatively higher noise margin and gain is maintained for CMOS configured hybrid biosensor than resistive load configurations that too for both types of devices (junctionless DM-FETs and inversion mode DM-FETs). The sensitivity for proposed hybrid biosensor is computed by observing relative change in logic threshold voltage (V_{Lt}) given by $|\frac{V_{Lt}(empty,K=1)-V_{Lt}(biosample,K)}{V_{Lt}(empty,K=1)}| \times 100\%$. Figure 9 shows the VTC's for cascaded two stage CMOS configured hybrid biosensor. This configuration shows the best DC gain among all configurations. Here the noise is eliminated in second stage due to CMOS topology. The observed values of gain (A_v), V_{Lt}, $\triangle V_{Lt}$, and sensitivity is shown in Table 3. A remarkable improvement in gain is observed in two stage hybrid biosensor compared to single stage and more importantly hybrid biosensors based on junctionless DM-FETs have relatively higher average sensitivity that its counterparts. The proposed hybrid biosensor offers a drastic sensitivity amplification of bio-signal response without additional off-chip circuitry. The high sensitivity shown by the proposed GAA-JL DMFET based hybrid biosensor supports its applicability to other biosample detections systems.

For any sensing metric used it is important the sensing device must yield a uniform or linear change in detecting electrical quantity for normalized change in the concentration of sensed biomatter. Linearity at the outset implies that the sensing metric (here change in logic threshold voltage) must satisfy the straight line equation ($y = mx+C$), where y denotes the change in logic threshold voltage, m denotes relative sensitivity, and C is the reference value of change in sensing metric at reference concentration (here K=1). The proposed architecture shows a good linear behavior for a dielectric constant range of 1(empty) to 3.57(APTES) as shown in Fig. 10. The linearity of any BioFET device depends on charge carrier concentration in silicon nanowire and thickness of the cavity. JL-DMFET BioFET based hybrid biosensor shows a better linearity with slope of 23.66 than that of IM-DMFET based hybrid biosensor with enhanced values of sensitivity.

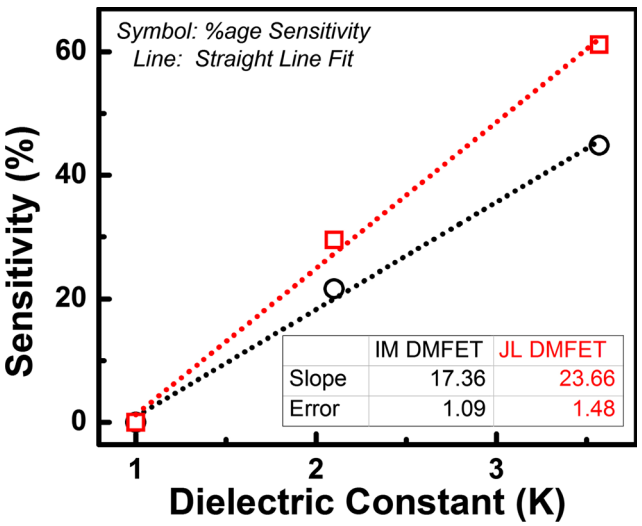

Fig. 10 Linearity for proposed hybrid biosensor based on inversion mode and junctionless BioFET. The inset table shows the slope and straight line fit errors for IM and JL DMFET baser hybrid biosensors

4 Conclusions and Future Work

Ultra sensitive, noise immune biosensors that can be monolithically integrated with amplifier and readout circuitry is future realm of miniaturized semiconductor biosensors that have superior performance that include large dynamic sensing range, minimal detection time, low operating voltage, low limit of lower detection and high integration density on chip. Such novel concept of hybrid biosensor design can be used to build autonomous miniaturized diagnostic devices. The results obtained establish the superiority of proposed gate all around junctionless DM-FET based hybrid biosensor over the similar configured topologies based on GAA conventional inversion mode DM-FET through extensive simulation results. The steeper VTCs of JL-DMFET based hybrid biosensor in comparison to conventional inversion mode DM-FET device based hybrid biosensor establish the superior noise performance of the former configuration. The performance of proposed concept of hybrid biosensing has been analyzed in terms of percentage shift in logic threshold voltage ($\triangle V_{Lt}$) and gain (A_V) considering the base case for empty cavity simulated by considering K=1. The proposed device based hybrid biosensor follows a good linear behavior with slope of 23.66 implying good sensitivity and very marginal error of 1.48 in the straight line fit. The topology of hybrid biosensor which involves two stage single sensing device with resistive load yields maximum $\triangle V_{Lt}$ sensitivity (61.14%) but suffers from poor total gain owed to passive load element in the pull up network. Gate all-round junctionless BioFET based hybrid biosensor yields as superior performance in cascaded CMOS configuration with $\triangle V_{Lt} \simeq 30\%$ and gain $A_V = 55$. Highest gain is achieved for two stage CMOS topology yielding almost a noise free output bioresponse. This advanced concept of hybrid biosensing has the potential of being extended to different BioFET architectures.

Compliance with Ethical Standards

Conflict of interests The authors declare that they have no conflict of interest.

References

1. Stern E, Vacic A, Reed MA (2008) IEEE Transactions on Electron Devices 55(11):3119. https://doi.org/10.1109/TED.2008.2005168
2. Gao Z, Agarwal A, Trigg AD, Singh N, Fang C, Tung CH, Fan Y, Buddharaju KD, Kong J (2007) Analytical Chemistry 79(9):3291. https://doi.org/10.1021/ac061808q
3. Shetti NP, Bukkitgar SD, Reddy KR, Reddy CV, Aminabhavi TM (2019) Biosensors and Bioelectronics 111417:141. https://doi.org/10.1016/j.bios.2019.111417
4. Shen MY, Li BR, Li YK (2014) Biosens Bioelectron 60:101. https://doi.org/10.1016/j.bios.2014.03.057
5. Voon CH, Sam ST (2019). In: Gopinath SC, Lakshmipriya T (eds) Nanobiosensors for biomolecular targeting, Micro and Nano Technologies. Elsevier, pp 23–50. https://doi.org/10.1016/B978-0-12-813900-4.00002-6
6. Bergveld P (2003) Sensors and Actuators B:, Chemical 88(1):1. https://doi.org/10.1016/S0925-4005(02)00301-5
7. Schöning M. J., Poghossian A (2002) Analyst 127:1137. https://doi.org/10.1039/B204444G
8. Chou JC, Hsiao CN (2000) Mater Chem Phys 63(3):270. https://doi.org/10.1016/S0254-0584(99)00188-1
9. Chou JC, Hsiao CN (2000) Sensors and Actuators B:, Chemical 66(1):181. https://doi.org/10.1016/S0925-4005(00)00341-5
10. Jakobson C, Feinsod M, Nemirovsky Y (2000) Sensors and Actuators B:, Chemical 68(1):134. https://doi.org/10.1016/S0925-4005(00)00473-1
11. Im H, Huang XJ, Gu B, Choi YK (2007) Nat Nanotechnol 2(7):430. https://doi.org/10.1038/nnano.2007.180
12. Shafi N, Sahu C, Periasamy C (2019) IEEE Electron Device Letters 40(6):997. https://doi.org/10.1109/LED.2019.2911334
13. Shafi N, Sahu C, Periasamy C (2020) IEEE Sensors Journal, 1–1. https://doi.org/10.1109/JSEN.2020.2964625
14. Kim C, Kim J, Moon D, Choi J, Choi Y (2016) IEEE Trans Nanotechnol 15(2):188. https://doi.org/10.1109/TNANO.2015.2512300
15. Gu B, Park TJ, Ahn JH, Huang XJ, Lee SY, Choi YK (2009) Small 5(21):2407. https://doi.org/10.1002/smll.200900450
16. Im M, Ahn J, Han J, Park TJ, Lee SY, Choi Y (2011) IEEE Sensors J 11(2):351. https://doi.org/10.1109/JSEN.2010.2062502
17. Kim C, Ahn J, Lee K, Jung C, Park HG, Choi Y (2012) IEEE Transactions on Electron Devices 59(10):2825. https://doi.org/10.1109/TED.2012.2209650
18. Ahn J. H., Choi S. J., Im M., Kim S., Kim C. H., Kim J. Y., Park T. J., Lee S. Y., Choi Y. K. (2017) Appl Phys Lett 111(11):113701. https://doi.org/10.1063/1.5003106
19. Shafi N, Sahu C, Periasamy C (2018) Superlattice Microst 120:75. https://doi.org/10.1016/j.spmi.2018.05.006
20. Colinge JP, Lee CW, Afzalian A, Akhavan ND, Yan R, Ferain I, Razavi P, O'neill B, Blake A, White M, et al. (2010) Nature Nanotechnology 5(3):225. https://doi.org/10.1038/nnano.2010.15
21. Su CJ, Tsai TI, Liou YL, Lin ZM, Lin HC, Chao TS (2011) IEEE Electron Device Letters 32(4):521. https://doi.org/10.1109/LED.2011.2107498
22. Buitrago E, Fagas G, Badia MFB, Georgiev YM, Berthomé M., Ionescu AM (2013) Sensors and Actuators B:, Chemical 183:1. https://doi.org/10.1016/j.snb.2013.03.028
23. Moon D, Choi S, Duarte JP, Choi Y (2013) IEEE Transactions on Electron Devices 60(4):1355. https://doi.org/10.1109/TED.2013.2247763
24. Kranti A., Yan R., Lee C., Ferain I., Yu R., Dehdashti Akhavan N., Razavi P., Colinge J. (2010) In: 2010 Proceedings of the European Solid State Device Research Conference, pp 357–360. https://doi.org/10.1109/ESSDERC.2010.5618216
25. Mukherjee C., Maneux C., Pezard J., Larrieu G. (2017) In: 2017 47th European Solid-State Device Research Conference (ESSDERC), pp 34–37. https://doi.org/10.1109/ESSDERC.2017.8066585
26. Jeon DY, Park SJ, Mouis M, Barraud S, Kim GT, Ghibaudo G (2013) Solid State Electron 81:101. https://doi.org/10.1016/j.sse.2012.12.003
27. Sahu C, Singh J (2014) IEEE Electron Device Letters 35(3):411. https://doi.org/10.1109/LED..2297451
28. Parihar MS, Ghosh D, Kranti A (2013) IEEE Transactions on Electron Devices 60(5):1540. https://doi.org/10.1109/TED.2013.2253324

29. Chandrasekaran AR (2017) Journal of Nanomaterials, 2017. https://doi.org/10.1155/2017/2820619
30. Ishige Y., Shimoda M., Kamahori M. (2009) Biosensors and Bioelectronics 24(5):1096. https://doi.org/10.1016/j.bios.2008.06.012. Selected Papers from the Tenth World Congress on Biosensors Shangai, China, May 14-16, 2008
31. Lee J., Jang J., Choi B., Yoon J., Kim J. Y., Choi Y. K., Myong D., Kim D, Kim H, Choi S. J. (2015) Scientific Reports 5:12286 EP. https://doi.org/10.1038/srep12286. Article
32. Lee J, Hwang S., Choi B, Lee J. H, Moon D, Seol M., Kim C., Chung I., Park B., Choi Y., Kim D. M., Kim D. H., Choi S. (2013) In: 2013 IEEE International Electron Devices Meeting, pp 14.5.1–14.5.4. https://doi.org/10.1109/IEDM.2013.6724631
33. Gao A, Zou N, Dai P, Lu N, Li T, Wang Y, Zhao J, Mao H (2013) Nano Lett 13(9):4123. https://doi.org/10.1021/nl401628y
34. Kanungo S, Chattopadhyay S, Sinha K, Gupta PS, Rahaman H (2017) IEEE Sensors J 17(5):1399. https://doi.org/10.1109/JSEN.2016.2633621
35. Clément N, Han XL, Larrieu G (2013) Appl Phys Lett 103(26):263504. https://doi.org/10.1063/1.4858955
36. Knopfmacher O, Tarasov A, Fu W, Wipf M, Niesen B, Calame M, Schönenberger C. (2010) Nano Lett 10(6):2268. https://doi.org/10.1021/nl100892y
37. Stern E, Klemic JF, Routenberg DA, Wyrembak PN, Turner-Evans DB, Hamilton AD, LaVan DA, Fahmy TM, Reed MA (2007) Nature 445(7127):519. https://doi.org/10.1038/nature05498